

# MODEL SELECTION IN ULTRASONIC MEASUREMENTS ON TRABECULAR BONE

Christian C. Anderson, M.A.<sup>\*</sup>, Karen R. Marutyan, Ph.D.<sup>†</sup>, Keith A. Wear Ph.D.<sup>\*\*</sup>, Mark R. Holland, Ph.D.<sup>\*</sup>, James G. Miller, Ph.D.<sup>\*</sup> and G. Larry Bretthorst, Ph.D.<sup>†</sup>

<sup>\*</sup>*Laboratory For Ultrasonics, Department of Physics, Washington University, St. Louis, MO 63130*

<sup>†</sup>*Biomedical Magnetic Resonance Laboratory, Mallinckrodt Institute of Radiology, Washington University, St. Louis, MO 63110*

<sup>\*\*</sup>*U.S. Food and Drug Administration, Center for Devices and Radiological Health, Silver Spring, MD 20993*

**Abstract.** Previous work from our laboratory showed that the widely reported decrease in phase velocity with frequency (negative dispersion) for ultrasonic waves propagating through trabecular bone can arise from the interference of two compressional waves, each of which exhibits a positive dispersion. Previous simulations suggest that Bayesian probability theory can be employed to recover the material properties linked to these two interfering waves, even when the waves overlap sufficiently that visual inspection cannot distinguish two modes. In the present study, Bayesian probability theory is applied first to simulated data and then to representative experimental bone data to determine whether one or two compressional wave modes are present. Model selection is implemented by evaluating the posterior probability for each model. The calculation is implemented by defining a model indicator and then using Markov chain Monte Carlo with simulated annealing to draw samples from the joint posterior probability for the ultrasonic parameters and the model indicator. Monte Carlo integration is used to evaluate the marginal posterior probability for each parameter given the model indicator.

## INTRODUCTION

Quantitative ultrasound has become an accepted modality to aid in the assessment of osteoporotic fracture risk. However, as outlined in a companion article [1], the interaction of ultrasound with trabecular (cancellous) bone is not well understood. In particular, the observed decrease of phase velocity with frequency (negative dispersion) in human calcaneus appears to be inconsistent with the requirements of causality. More specifically, the causality-based Kramers-Kronig relations that relate attenuation to dispersion suggest that media with a linear-with-frequency increase in attenuation coefficient should show an increase in phase velocity with frequency (positive dispersion) [2]. Because bone has been demonstrated to have an approximately linear- or quasilinear-with-frequency increase in attenuation coefficient [2, 3], the observed negative dispersion is perplexing.

Our laboratory recently proposed a hypothesis to explain the observed negative dispersion in human calcaneus—namely, that received signals are not comprised of one propagating compressional wave, but are instead a superposition of two overlapping compressional waves, a fast wave and a slow wave [4]. In this view, the individual fast and

slow waves exhibit positive dispersion in accordance with the Kramers-Kronig relations, but interfere in such a way as to produce a waveform with an apparent negative dispersion when analyzed conventionally under the assumption that one wave is present. The true ultrasonic properties of bone, as represented by the properties of the fast and slow waves, could provide more diagnostically relevant information than the apparent properties (e.g. negative dispersion) obtained through conventional means. The propagation of two compressional waves through trabecular bone has been observed experimentally [5] and predicted theoretically [6, 7].

Bayesian probability theory shows promise in recovering the properties of individual superposed waves [8]. The companion article [1] addresses the parameter estimation problem involving ultrasonic measurements on trabecular bone. In that work, Bayesian inference methods are used to recover the properties of simulated waveforms generated through the superposition of fast and slow waves. In the current article, we apply Bayesian probability theory to the model selection problem; that is, the problem of determining whether the received waveforms are composed of one wave or two interfering waves.

## ULTRASONIC PROPAGATION MODELS

In a typical ultrasound experiment, two cylindrical ultrasonic transducers are immersed in water and coaxially aligned; one acts as a transmitter, and the other acts as a receiver. Data are acquired with and without a sample placed between the transducers. Since water is a well-characterized medium, analysis on the sample proceeds by referencing the signal that travels through the sample to the signal that travels only through water (the reference water-path signal).

Although acquired ultrasonic signals generally consist of time-domain data, we are concerned with properties that are conveniently analyzed in the frequency domain (i.e., frequency-dependent attenuation and dispersion). Accordingly, our ultrasonic propagation models are designed using a frequency-domain approach and act on the discrete Fourier transforms of the input data. The propagated frequency spectra are converted back to temporal signals to provide an intuitive representation of the acquired waveform.

Following the convention in [1], we model the received data as

$$d_i = \text{Real} \left[ \frac{1}{N} \sum_{j=1}^N P_j \exp(-i\omega_j t_i / N) \right] + n_i \quad (1)$$

where  $d_i$  is a real data value sampled at time  $t_i$ ,  $P_j$  represents a value of the propagated complex spectrum at angular frequency  $\omega_j$ ,  $N$  is the number of points in the frequency-domain representation of the data, and  $n_i$  is additive noise.

At this point, we depart from the notation used in [1], because that article assumes that two compressional ultrasonic waves propagate through bone. Here, we evaluate whether individual received signals are composed of one or two compressional waves. In this treatment, the propagated spectra,  $P_j$  in Eq. (1), depend on the respective models for ultrasonic propagation through bone. In the models considered here, the transmitted

signals and the received propagated signals are related by mathematical representations known as transfer functions. The  $P_j$  are of the form

$$P_j = A_j \sum_{z=1}^m H_{z,j} \quad (2)$$

where  $A_j$  is the complex spectrum of the ultrasonic pulse before it encounters the bone specimen,  $m$  is the number of wave modes present in the model, and  $H_{z,j}$  is the  $z$ th transfer function for the propagation model. The one-mode model has one associated transfer function ( $m = 1$ ), whereas the two-mode model involves two transfer functions ( $m = 2$ ). For linear plane wave propagation,  $H_{z,j}$  is given as

$$H_{z,j} = S_z \exp(-\alpha_{z,j}l) \exp\left(-i\omega_j \frac{l}{v_{z,j}}\right) \quad (3)$$

where  $S_z$  is an amplitude scaling parameter representing frequency-independent loss,  $l$  is the specimen thickness,  $\alpha_{z,j}$  is the attenuation coefficient, and  $v_{z,j}$  is the phase velocity at frequency  $\omega_j$ . If we assume that the attenuation coefficient rises linearly with frequency,  $\alpha_{z,j}$  becomes

$$\alpha_{z,j} = \beta_z \frac{\omega_j}{2\pi}. \quad (4)$$

The parameter  $\beta_z$  is commonly known in the tissue characterization community as the ‘‘slope of attenuation,’’ while in the bone literature it is referred to as ‘‘normalized Broadband Ultrasound Attenuation (nBUA).’’

The phase velocities  $v_{z,j}$  are of the form

$$v_{z,j} \approx v_z + \frac{\beta_z}{\pi^2} v_z^2 \ln\left(\frac{\omega_j}{\omega_r}\right) \quad (5)$$

where  $v_z$  is a phase velocity at some arbitrarily chosen reference angular frequency  $\omega_r$  [4]. The value of the reference frequency is chosen based on the spectral characteristics of the interrogating ultrasonic pulse. Equation (5) is consistent with the causality-imposed Kramers-Kronig relations for media with an attenuation coefficient of the form in Eq. (4).

## BAYESIAN CALCULATIONS

The goal of model selection problems is to calculate the posterior probability for the model, conditional on the input data and background information. To accomplish this calculation, a model indicator  $u$  is introduced. Two models are considered here, so we constrain the possible values of  $u$  to  $\{1, 2\}$ , where  $u = 1$  corresponds to the hypothesis, ‘‘the received data are described by a one-mode propagation model,’’ and  $u = 2$  represents the hypothesis, ‘‘the received data are described by a two-mode propagation model.’’ The posterior probability for the model indicator can now be written  $P(u|DI)$ , where  $D$  is

the data and  $I$  is the background information. The posterior probability for the model indicator is computed by the application of Bayes' theorem

$$P(u|DI) = \frac{P(u|I)P(D|uI)}{P(D|I)}. \quad (6)$$

The term  $P(u|I)$  in Eq. (6) is the prior probability for the model indicator, and  $P(D|uI)$  is the marginal direct probability for the data given the model indicator and background information. The probability for the data given the background information,  $P(D|I)$ , is a normalization constant. If we normalize Eq. (6) at the end of the calculation, then the equality becomes a proportionality

$$P(u|DI) \propto P(u|I)P(D|uI). \quad (7)$$

The direct probability for the data given the model indicator,  $P(D|uI)$ , is a marginal probability because it does not contain any model parameters. Reintroducing these parameters, the marginal direct probability can be computed by application of the sum and product rules:

$$P(D|uI) = \int d\Theta_u P(\Theta_u D|uI), \quad (8)$$

in which  $\Theta_u$  represents the parameters for model  $u$ . In the models for ultrasonic wave propagation, there are three unknown parameters for each wave:  $S_z$ ,  $v_z$ , and  $\beta_z$  in Eqs. (3-5). Thus, when  $u = 1$ , the integral in Eq. (8) is three-dimensional, and when  $u = 2$ , it is six-dimensional. The joint probability for the parameters and the data,  $P(\Theta_u D|uI)$ , can be factored using the product rule of probability theory; Eq. (8) becomes

$$P(D|uI) = \int d\Theta_u P(\Theta_u|uI)P(D|\Theta_u uI), \quad (9)$$

where  $P(D|\Theta_u uI)$  is the probability for the data given the model indicator, parameters for the indicated model, background information and  $P(\Theta_u|uI)$  is the prior probability for the model parameters given the model indicator and background information. Substituting Eq. (9) into Eq. (7), we arrive at an expression for the posterior probability for the model indicator,

$$P(u|DI) \propto P(u|I) \int d\Theta_u P(\Theta_u|uI)P(D|\Theta_u uI), \quad (10)$$

where terms of the form  $P(\Theta_u|uI)P(D|\Theta_u uI)$  are, up to a normalization constant, the joint posterior probability for the parameters given the model indicator. These calculations are given in [1], and we do not repeat them here.

We now turn our attention to assigning the prior probability for the model indicator,  $P(u|I)$ . Before performing any calculations, we have no reason to prefer the two-mode model over the one-mode model (or vice versa), so we assign a flat (uniform) distribution to reflect this state of knowledge.

Integrals such as the one in Eq. (10) rarely have analytic solutions, and numerical methods must therefore be employed to determine the posterior probability for the model indicator. The method used here is Markov chain Monte Carlo with simulated annealing [9].

## DISCUSSION

A broadband ultrasonic pulse was experimentally acquired using paired transducers in a water bath. The nominal center frequency of the transducers was 500 kHz, and the -6 dB bandwidth limits of the pulse spanned the approximate frequency range 280-640 kHz. At this frequency range, propagation of the pulse through water was assumed to have a negligible effect on its attenuation and dispersion characteristics. The pulse was altered using the models described above to simulate one-mode propagation and two-mode propagation through a bone sample. The parameters used to generate the waveforms were selected so that the simulated data were qualitatively similar to experimentally acquired data. The simulated one-mode waveform was generated with  $\{S_1, \beta_1, v_1\} = \{0.7, 30 \text{ Np/m/MHz}, 1500 \text{ m/s}\}$ , and the simulated two-mode waveform was generated with  $\{S_1, \beta_1, v_1; S_2, \beta_2, v_2\} = \{0.6, 30 \text{ Np/m/MHz}, 1500 \text{ m/s}; 0.3, 50 \text{ Np/m/MHz}, 1600 \text{ m/s}\}$ . In both cases, the values of  $l$  and  $\omega_r/2\pi$  were 1.85 cm and 500 kHz, respectively. Additive Gaussian noise with a signal-to-noise ratio of 50:1 was incorporated into the simulated waves, which were used as inputs to the Bayesian analysis program. The original, unaltered water-path pulse served as a reference signal.

Bayesian inference was also applied to experimental data obtained by interrogating 24 human calcaneus samples with ultrasound. These data were acquired with the same transducers used to generate the pulse described above. A more complete description of the experimental methodology can be found elsewhere [10]. Conventional phase spectroscopy analysis of the received signals revealed that a large majority of the samples exhibited negative dispersion.

In the program that implements this calculation multiple Markov chain Monte Carlo simulations are run simultaneously and in parallel. Each of these simulations has a model indicator that has value 1 or 2. One of the steps in the Monte Carlo simulation is to propose a new model indicator. Consequently, the number of simulations having model indicator 1 or 2 changes as a function of the annealing parameter. When the simulations begin, the annealing parameter is zero, the data are being ignored. So the number of simulations having model indicator 1 or 2 reflects the prior probability. The prior is uniform, so the number of simulations having a one-mode model is roughly equal to the number of simulations having a two-mode model. This effect is illustrated in Fig. 1 where the fractions of Markov chain Monte Carlo simulations having model indicator equal to 1 is plotted in gray as a function of the annealing parameter  $\beta$ . Similarly, the fractions of simulations having model indicator equal to 2 are plotted in black. In panel **a**, the synthetic data were generated with a model containing one-mode. As the annealing parameter increases, the simulations transition to the one-mode model because, for all practical purposes, the one and two-mode models have equal likelihoods, but all the additional parameters in the two-mode model reduce its posterior probability. However, in panel **b**, the synthetic data contain two wave modes. It is illustrated in [1] that when data containing two-modes is analyzed using a single mode model, the residuals generated from the parameters that maximize the posterior probability contain large systematic artifacts. Because the mean-square residual is essentially the negative logarithm of the likelihood, larger systematic variations in the residuals means a lower likelihood; and, consequently, the posterior probability for the one-mode model is much lower than the posterior probability for the two-mode model. This effect is illustrated

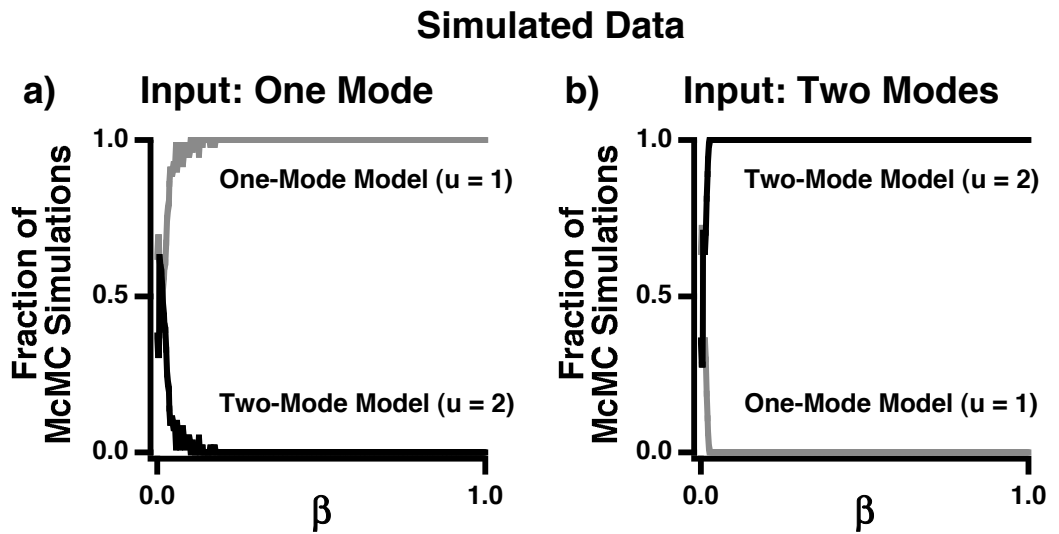


**FIGURE 1.** The fractions of Markov chain Monte Carlo simulations having model indicator equal to 1 (gray) and 2 (black) is plotted as a function of the annealing parameter  $\beta$ . As  $\beta$  increases, the simulations transition to the one-mode model when the data consist of one mode (panel **a**) and to the two-mode model when the data consist of two modes (panel **b**).

in panel **b** where there is a very sharp transition to the two-mode model because a one-mode model cannot fit the data. Note this transition is much sharper than the transition in panel **a** where it is the prior probabilities that force the transition to the one-mode model.

Figure 2 illustrates the results of the analysis when simulated one, two and real experimental data are analyzed, panels **a**, **b** and **c** respectively. The simulated signals appear in panels **a** and **b**, and a single representative signal propagated through human calcaneus is shown in panel **c**. Panels **d**, **e**, and **f** are output waveforms constructed from the parameters that maximized the joint posterior probability for the parameters and the model indicator. When simulated one-mode data are input, the one-mode model is selected. When a two-mode waveform is the input, the two-mode model is selected. In both instances, the residuals (panels **g** and **h**) are random and on the order of the noise in the input data. When an experimentally acquired data set is analyzed, the two-mode model is selected. However, systematic variations are apparent in the residuals (panel **i**). Similar results were obtained for all experimentally acquired signals. The artifacts in the residuals imply that the wave propagation models presented earlier are only an idealized, approximate representation of actual ultrasound propagation through bone. Indeed, several factors related to the experimental design, including but not limited to beam diffraction, phase cancellation at the face of a phase sensitive receiver, and issues relating to transmission and reflection at the tissue-water interface, are not fully incorporated into the propagation models. Consequently, further study is necessary to determine conclusively if the two-mode hypothesis is a preferred alternative to other explanations of the observed negative dispersion in bone.

Despite the apparent incompleteness of the current model for two-mode propagation,

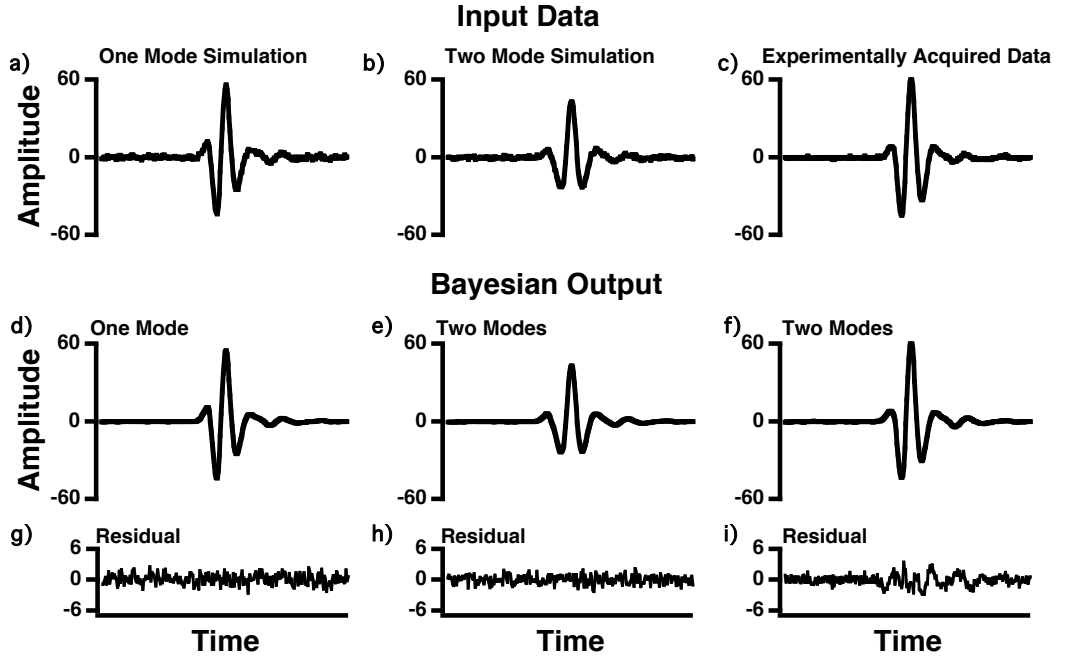


**FIGURE 2.** Panels **a** and **b** show simulated one and two-mode data, while panel **c** is experimental data. Panels **d**, **e**, and **f** are the models generated from the parameters that maximized the joint posterior probability for the parameters and the model indicator given each of the three data sets. For the one and two-model simulated data, the program correctly identifies the number of modes and generates residuals that model the data down to the noise, panels **g** and **h**. However, the residuals generated from the experimental data, panel **i**, show systematic artifacts even for the two-mode model.

it appears to be more capable of recovering the frequency dependence of phase velocity than a one-mode model. This is illustrated in Fig. 3 where the dispersion computed from experimental and simulated data are shown. These dispersion curves are computed from the following equation

$$v_{phase}(\omega) = \frac{v_{water}}{1 - \frac{v_{water}}{d} \frac{\Delta\phi(\omega)}{\omega}} \quad (11)$$

where  $v_{phase}(\omega)$  is phase velocity at frequency  $\omega$ ,  $v_{water}$  is speed of sound in water,  $d$  is sample thickness,  $\Delta\phi(\omega)$  is the difference in phase between the reference signal and through-sample signal. It is calculated by Fourier transforming the reference and sample signals, computing the phase and then taking the difference. The dispersion curves for the experimental data are shown as the gray curves in panels **a** and **b**. This experimental data was then analyzed using a one and two-mode model. The parameters that maximized the joint posterior probability were then used to generate simulated data and these simulations were then used to compute the dispersion curves. The dispersion curves computed from the simulated one and two -mode models are shown as the black curves in panels **a** and **b** respectively. The dispersion curves for the experimental data show negative dispersion, while the dispersion curves computed from the one-mode model are positive. However, the dispersion curve computed from the two-mode model show negative dispersion; even though the individual fast and slow waves each show a

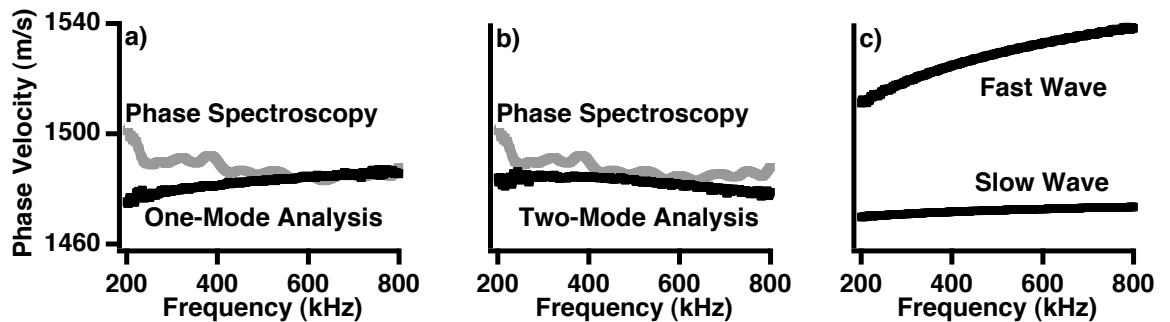


**FIGURE 3.** The experimental data was analyzed using both a one-mode and two-mode model. The parameters that maximized the joint posterior probability for a one-mode and a two-mode model were used to generate simulated data. Dispersion curves were then computed for these simulated and experimental data sets, see text for this calculation. The dispersion curves generated from the one-mode model are always positive, black curves in **a**; while the experimental data exhibit negative, decreasing, dispersion (gray curves in panels **a** and **b**). However, the dispersion curves generated from the two-mode model produces a negative dispersion (black curve in panel **b**), even though the individual fast and slow waves that compose the two-mode waveform exhibit positive dispersion (**c**).

positive dispersion (panel **c**). Throughout the usable bandwidth (approximately 280-640 kHz), the agreement between the phase spectroscopy analysis on the two-mode model and the experimental data is quite good, especially in regard to the frequency dependence of phase velocity.

## SUMMARY

We have addressed the question of the number of wave modes present in simulated and experimental data from signals transmitted through trabecular bone using Bayesian probability theory. A program that implements the Bayesian calculations accurately determined the number of wave modes present in simulated data, and preferred the two-mode propagation model to describe experimentally obtained signals transmitted through human calcaneus. The models for ultrasonic propagation require further refinement if definitive conclusions about ultrasonic propagation through bone are to be drawn. Nevertheless, Bayesian probability theory shows promise as an effective method of evaluating different ultrasonic propagation models.

## REFERENCES

1. Marutyan, K.R., Anderson, C.C., Wear, K.A., Holland, M.R., Miller, J.G. and Bretthorst, G.L. (2007). Parameter estimation in ultrasonic measurement on trabecular bone. Ed. Mohammad-Djafari A, Maximum entropy and Bayesian methods in science and engineering, in this issue.
2. Waters, K.R. and Hoffmeister, B.K. (2005). Kramers-Kronig analysis of attenuation and dispersion in trabecular bone. *J Acoust Soc Am*, 118(6):3912–3920.
3. Droin, P., Berger, G. and Laugier, P. (1998). Velocity dispersion of acoustic waves in cancellous bone. *IEEE Trans Ultrason Ferroelectr Freq Control*, 45(3):581–592.

4. Marutyan, K.R., Holland, M.R. and Miller, J.G. (2006). Anomalous negative dispersion in bone can result from the interference of fast and slow waves. *J Acoust Soc Am*, 120(5):EL55–61.
5. Hosokawa, A. and Otani, T. (1997). Ultrasonic wave propagation in bovine cancellous bone. *J Acoust Soc Am*, 101(1):558–562.
6. Haire, T. and Langton, C. (1999). Biot theory: A review of its application to ultrasound propagation through cancellous bone. *Bone*, 24(4):291–295.
7. Hughes, E.R., Leighton, T.G., Petley, G.W. and White, P.R. (1999). Ultrasonic propagation in cancellous bone: a new stratified model. *Ultrasound Med Biol*, 25(5):811–821.
8. Marutyan, K.R., Bretthorst, G.L. and Miller, J.G. (2007). Bayesian estimation of the underlying bone properties from mixed fast and slow mode ultrasonic signals. *J Acoust Soc Am*, 121(1):EL8–15.
9. Bretthorst, G.L., Hutton, W.C., Garbow, J.R. and Ackerman, J.J. (2005). Exponential model selection (in NMR) using Bayesian probability theory. *Concepts in Magnetic Resonance*, 27A:64–72.
10. Wear, K.A. (2000). Measurements of phase velocity and group velocity in human calcaneus. *Ultrasound Med Biol*, 26(4):641–646.